Photocatalysis

How to cite:
International Edition: doi.org/10.1002/anie.202208611
German Edition: doi.org/10.1002/ange.202208611

Hydrogen-Bond-Modulated Nucleofugality of Se^{III} Species to Enable Photoredox-Catalytic Semipinacol Manifolds

Sooyoung Park[+], Amit K. Dutta[+], Carina Allacher, Anton Abramov, Philipp Dullinger, Katerina Kuzmanoska, Daniela Fritsch, Patrick Hitzfeld, Dominik Horinek, Julia Rehbein, Patrick Nuernberger,* Ruth M. Gschwind,* and Alexander Breder**

In memory of Professor Ulf Diederichsen

Abstract: Chemical bond activations mediated by H-bond interactions involving highly electronegative elements such as nitrogen and oxygen are powerful tactics in modern catalysis research. On the contrary, kindred catalytic regimes in which heavier, less electronegative elements such as selenium engage in H-bond interactions to co-activate C–Se σ-bonds under oxidative conditions are elusive. Traditional strategies to enhance the nucleofugality of selenium residues predicate on the oxidative addition of electrophiles onto Se^{II}-centers, which entails the elimination of the resulting Se^{IV} moieties. Catalytic procedures in which Se^{IV} nucleofuges are substituted rather than eliminated are very rare and, so far, not applicable to carbon-carbon bond formations. In this study, we introduce an unprecedented combination of O–H···Se H-bond interactions and single electron oxidation to catalytically generate Se^{III} nucleofuges that allow for the formation of new C–C σ-bonds by means of a type I semipinacol process in high yields and excellent selectivity.

Introduction

The use of hydrogen bond interactions (H-bonds) for the selective activation of specific chemical bonds to create a desired reactivity pattern at a given site within a substrate ranks among the key mechanistic tactics in modern catalysis research.[1,2] In most of such applications, H-bonds are harnessed for (1) their capacity to alter the polarity of the bonds adjacent to the donor (D) and acceptor (A) atoms between which the H-bond is formed (i.e., E–D–H···A–E′; E/E′ = any given elements) and (2) their spatial directionality, which typically results in a well-defined assembly of the H-bond donor/acceptor components.[3–5] While most of the second row p-block elements such as carbon, nitrogen, oxygen, and fluorine have found use as donors and/or acceptors in H-bond assisted catalysis,[6] there are virtually no reports on cognate processes involving the heavier group 16 homologs such as selenium to serve as a H-bond acceptor (i.e., D–H···Se) and activate, for instance, appendant selenium-carbon bonds. The inobservance of the immense synthetic potential is partly due to the doctrine that selenium-centered H-bonds are generally weak and therefore negligible compared to those derived from more electronegative acceptors such as oxygen and nitrogen. However, Biswal et al. were able to show by high resolution vibrational spectroscopy and quantum chemical calculations that selenium and even tellurium can sustain H-bonds with amide donors that are equal or even higher in strength than oxygen.[7,8] The authors rationalized their findings with a decreasing contribution of electronegativity to the overall strength of D–H···A H-bonds (A = chalcogens) when going from oxygen down to tellurium. However, this energetic loss is (over)compensated with a steadily increasing contribution by atomic polarizability and dispersion energy down along the group 16 elements.[9] In addition, selenium was shown to display a profuse array of H-bond interactions in the context of molecular biology, structural chemistry, and functional materials.[7–10] Against this background, we posited that

[*] S. Park,[+] A. K. Dutta,[+] A. Abramov, P. Dullinger, K. Kuzmanoska, D. Fritsch, P. Hitzfeld, J. Rehbein, R. M. Gschwind, A. Breder
Institut für Organische Chemie, Universität Regensburg
Universitätstrasse 31, 93053 Regensburg (Germany)
E-mail: julia.rehbein@chemie.uni-regensburg.de
ruth.gschwind@chemie.uni-regensburg.de
alexander.breder@chemie.uni-regensburg.de

C. Allacher, D. Horinek, P. Nuernberger
Institut für Physikalische und Theoretische Chemie, Universität Regensburg
Universitätstrasse 31, 93053 Regensburg (Germany)
E-mail: patrick.nuernberger@chemie.uni-regensburg.de

[+] These authors contributed equally to this work.

D–H···Se H-bonds may have a significant impact on the nucleofugality of selenium residues and that this feature may be harnessed in catalytic reactions. A prevalent mechanistic feature of alkyl(aryl)selanes is their tendency to undergo elimination reactions upon oxidative addition of electrophiles to Se^{II} centers (Scheme 1, path a, top right).[11] However, initial reports by Ward et al. and later by Engman showed that the chemoselectivity toward elimination can be altered into S_N2-manifolds when suitable nucleophiles are present in sufficient concentrations during the formation of the hypervalent Se^{IV} intermediate (Scheme 1, path b, middle right).[11–13] This notion led to sporadic reports on stoichiometric *cis*-1,2-difunctionalizations such as dihalogenations.[11–13] More recently, Denmark et al. and Michael et al. further expanded on this concept by developing catalytic protocols that enabled the direct and, in part, asymmetric *syn*-1,2-dichlorination, *syn*-1,2-oxyamination, and *syn*- as well as *anti*-1,2-diamination of alkenes, respectively.[14–17] Drawing a conceptual analogy between hypervalent Se^{IV} nucleofuges and hydrogen bonded Se^{II}-centers as discussed above, two key questions arise: 1) can D–H···Se H-bonds be harnessed to modulate the nucleofugality of selenium leaving groups—for instance, generated by single electron oxidation (i.e., Se^{III} nucleofuges)—to enable substitutions rather than eliminations and 2) can this H-bond-modulated nucleofugality be implemented in such a way that new carbon-carbon bonds are formed (Scheme 1, bottom right)? As a consequence of these considerations, we disclose herein an unprecedented photoredox catalytic migratory fragmentation of selenohydrins to give a broad panoply of α-branched carbonyl compounds.

Results and Discussion

Selenohydrins were identified as ideal candidates to study the hypothesized modulatory influence of O–H···Se H-bonds on the nucleofugality of Se-residues. Pioneering work by Krief et al. (Scheme 2a) and Paquette et al. showed that selenohydrins can undergo type I semipinacol rearrangements[18] if specific criteria are fulfilled: a) activation of the Se-residue had to take place covalently and stoichiometrically via *Se*-(dichloro)alkylation, b) as stated by Krief et al., the Se-nucleofuge has to be located at a tertiary C-atom for the rearrangement to take place,[19] c) the reaction was mechanistically dependent on the presence of bases with halophilic counterions such as thallium(I) or silver(I) cations.[20,21]

To evaluate whether the desired rearrangement described in Schemes 1b and 2b can be initiated by the combination of H-bond interactions and single electron oxidation, our first goal was to confirm the posited intramolecular O–H···Se contact by in-depth nuclear magnetic resonance (NMR) spectroscopy. Typically, changes of ^1H chemical shifts in response to additives or temperature are used as an indicator for the presence of H-bonds. However, chemical shift changes can also result from other causes.

Consequently, magnetization transfer through the partial covalent character of the putative O–H···Se H-bond was selected as a direct and unambiguous analytical method to corroborate its existence. Such magnetization transfers by scalar coupling (^hJ) along hydrogen-bonds directly pinpoint and interrelate their donor and acceptor atoms. So far, this technique has been applied only to bio-macromolecules[22,23] and very strong H-bonds in small molecules at low temperature,[24–26] as sufficient H-bond lifetimes in combina-

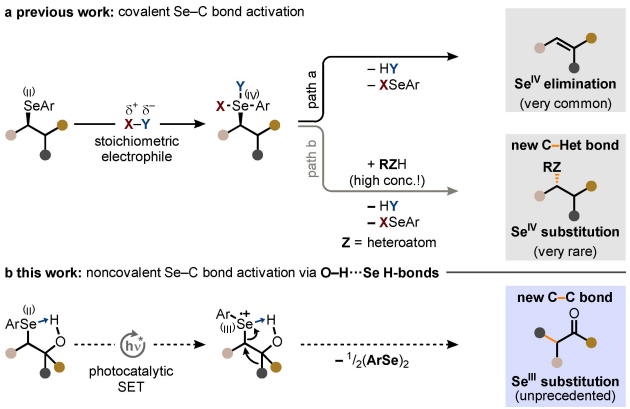

Scheme 1. Traditional stoichiometric, covalent nucleofugality enhancement of selenium residues via $Se^{II/IV}$ activation vs. non-covalent, H-bond-modulated nucleofugality enhancement via catalytic $Se^{II/III}$ activation (this work). a) Se^{IV} nucleofuges typically undergo rapid elimination (top right) or—in rare cases—substitution with heteroatomic nucleophiles either in high concentrations or intramolecularly (middle right). b) this work: unprecedented substitution of Se^{III} species with concomitant C–C bond formation (bottom right).

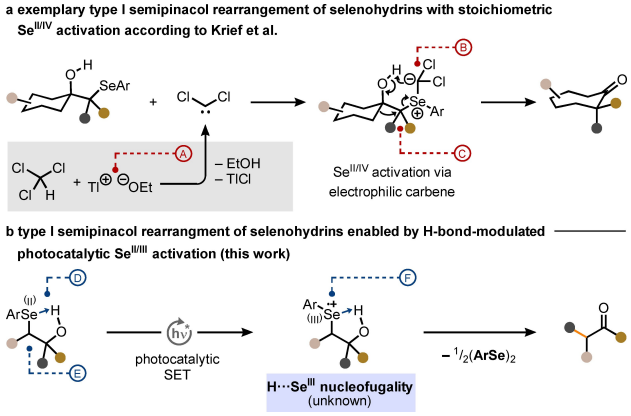

Scheme 2. Type I semipinacol rearrangement of selenohydrins actualized by classical covalent $Se^{II/IV}$ activation vs. H-bond-modulated, photoredox catalytic $Se^{II/III}$ activation (this work). a) Characteristics of classical approaches exemplified in the dichloromethylation of Se residues according to Krief et al.: A) bases with halophilic counterions are required, B) Se-group requires (super)stoichiometric activation with external electrophile, C) only tertiary carbon centers result in rearrangements. b) Characteristics of this approach: D) Se-group already pre-activated by O–H···Se H-bond, E) broader substitution pattern at the selenenylated sp^3-carbon atom tolerated, F) selenium group only requires photoredox catalytic activation.

tion with a partial covalent bonding character are required. To our knowledge, a magnetization transfer along a H-bond involving Se-acceptors is unreported so far. Therefore, based on our experience in H-bond analysis,[24,26–28] we selected selenohydrin **1a** (Scheme 3a,d) in neat dichloromethane-d_2 (DCM) as a model system, which was considered to provide maximum H-bond stabilization by a sterically fixed central five-membered ring and the lack of competing H-bond acceptors from the solvent (Scheme 3a). To our delight, in both 1D ^{1}H, ^{77}Se HSQC and 2D ^{1}H, ^{77}Se HMBC spectra an unusually intense cross peak between the OH and Se was detected (Scheme 3a,b), indicating a strong and stable O–H···Se H-bond even at room temperature. Analysis of the overall $J_{H,Se}$ intensity pattern clearly shows a magnetization transfer along the H-bond, dominantly actualized through scalar couplings (see Supporting Information).[22,24] Two derivatives of **1a**, namely selenohydrins **1b** and **1v** (Scheme 3e), showed nearly identical key signals in the NMR spectra. Since preliminary experiments showed that the aspired title reaction (Scheme 1b) proceeds in neat HFIP, the influence of this solvent on the OH···Se H-bond in **1a** was investigated, using 1, 2, and 3 equivalents of HFIP, respectively. The decision to use at most 3 equivalents of HFIP was taken based on reports by Berkessel et al. showing that up to 3 HFIP molecules can have a cumulative and thus distinct impact on H-bonds (Scheme 3a).[29] NMR spectra with 1–3 equivalents of HFIP showed a close contact but no influence on the OH···Se H-bond strength (Supporting Information). Next, we investigated whether the high strength of the O–H···Se H-bond might result from a strong conformational bias caused by the large substituents in **1a**. However, even **1a°**, which possesses an ethylene chain between the O and Se atom, provided similarly intense magnetization transfers along the O–H···Se H-bond, indicating that intrinsically strong O–H···Se H-bonds are generally present in selenohydrins—at least in DCM (Scheme 3c).

As mentioned before, up to 3 equivalents of HFIP did not affect the key H-bond in the NMR spectra. It was therefore interesting to analyze whether any changes of this intramolecular H-bond would occur in neat HFIP. Unfortunately, this medium produced extremely broad linewidths of the OH protons, preventing direct NMR investigations in this solvent. Therefore, we performed molecular dynamic (MD) simulations to check both the conformation and the effect of neat HFIP in comparison to CD_2Cl_2 as the solvent. For **1a** indeed a rigid, envelope-like ring system was found, which consists of the OH group, the selenium atom, and the two joining C atoms (Scheme 3d). The distance between the Se atom and the hydroxyl proton as well as the O–H···Se bond angle revealed an arrangement typical for a hydrogen bond interaction, thus corroborating the results of the NMR spectroscopic analysis (Supporting Information, Figure S4). In addition, a fixed orientation of the hydroxyl proton towards the Se center was detected,[30] i.e. the rotation of the OH group is not feasible even at 300 K and in neat HFIP (Supporting Information, Figures S3–S8). Next, the rotation around the OH-bond was simulated for selenohydrins **1a**, **1a**†, **1a**$^{\mp}$, and **1a°**, as they significantly differ from one

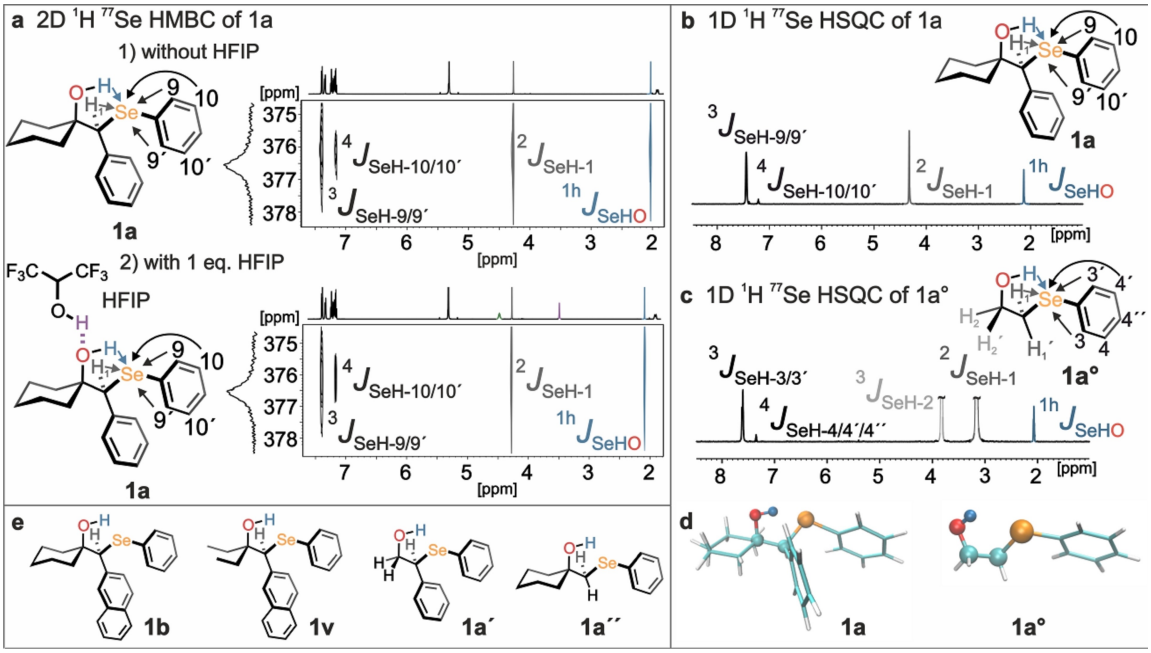

Scheme 3. Through H-bond magnetization transfers in 1D and 2D ^{1}H ^{77}Se heteronuclear NMR spectra reveal a stable ^{1}H ^{77}Se H-bond pattern with significantly covalent character. A) without HFIP (1) and with HFIP (2) similar cross peaks due to $^{1h}J_{SeHO}$ magnetization transfer (blue signal) are observed, indicating an anomalously strong OH–Se H-bond not influenced by 1 equiv of HFIP. B/C) 1D ^{1}H ^{77}Se HSQC spectra show that scalar coupling is the dominant origin for the magnetization transfer (for other contributions, see Supporting Information). Similar $^{1h}J_{SeHO}$ transfer intensities of **1a** and **1a°** indicate a negligible influence of sterics and conformational freedom on the H-bond peak. D) geometry of the OH–Se H-bonds in **1a** and **1a°** from MD snapshots. E) a stable H-bond pattern and geometry was observed via NMR for **1b** and **1v** and via MD for **1a**′ and **1a**″ (for data, see Supporting Information).

another in terms of steric constraints—with **1a** being most encumbered to **1a°** being most flexible (Scheme 3d). For all selenohydrins **1a**, **1a**†, **1a**$^{+}$, **1a°** (Schemes 3d,e, and S8b), similar minimum energy orientations of H towards Se were found. In addition, a second orientation with the OH pointing away from Se exists for all 4 systems. However, the free energy for this latter orientation is highest for **1a**, followed by **1a**†, and **1a**$^{+}$, and seems to be low enough only for **1a°** to be adopted. It is noteworthy that the force field MD simulations do not include any covalent Se–H contributions, which were shown to be significant and nearly identical for all substitution patterns in the NMR experiments. Therefore, the differences in conformational stability indicated by the MD simulations compared to the consistent NMR spectroscopic outcomes are best explained by the covalent character of the OH···Se H-bond. In conclusion, both NMR investigations and MD simulations consistently show that the OH···Se H-bond is by far stronger and more covalent than previously estimated. This notion suggests that a well-designed activation of Se moieties via H-bonds should be feasible for a very broad range of substrates.

Investigations continued with the identification of suitable reaction parameters to trigger the aspired type I semipinacol rearrangement photocatalytically and under H-bond assistance (Scheme 4). Previous studies showed that photoexcited tris(4-anisyl)pyrylium tetrafluoroborate (TAPT) possesses a sufficient redox potential (+1.84 V vs. SCE in MeCN) to oxidize alkyl(aryl)selanes (1.17–1.70 V vs. SCE in MeCN).[31,32] Therefore, **1a** was exposed to 5 mol % of TAPT at 465 nm irradiation in different organic solvents (0.1 M). Formation of **2a** was monitored by ^{1}H NMR spectroscopy and showed a significant correlation with the hydrogen-bond donor ability of the solvent—expressed as the Kamlet-Taft α-parameter (Scheme 4, red bars, dotted line).[33,34] For instance, only 3 % crude yield were recorded in *N*,*N*-dimethylformamide (α = 0.0) as a solvent, whereas HFIP (α = 1.96) furnished ketone **2a** in 75 %. No such correlation was found for other electronic solvent parameters, such as relative permittivity or dipole moment. We speculate that solvent-based H-bonds may have a decisive complementary impact on the rate of product formation in addition to the intramolecular H-bonds, as indicated by our NMR investigations (Scheme 3a). This hypothesis was supported by the fact that there was significant background reactivity (81 % conversion) at 465 nm in the absence of any photocatalyst, suggesting that the productive reaction pathway gradually becomes more dominant with an increasing H-bond donor ability of the solvent. To suppress any background processes, we screened for alternative photocatalysts that absorb at longer wavelengths but still sustain the title reaction. To this end, rose bengal (RB, with or without cinnamic acid, Scheme 4) as well as mono- (RBME) and dimethylated (DMRB) rose bengal derivatives proved most efficient (Scheme 4), which could be used at 530 nm and furnished target compound **2a** in yields of up to 87 %. Notably, in the absence of any photocatalyst at 530 nm, the conversion and crude yield were reduced to 4 % and 3 %, respectively. The conversion was also suppressed in the dark or absence of air, indicating that both parameters are crucial for the catalytic process.

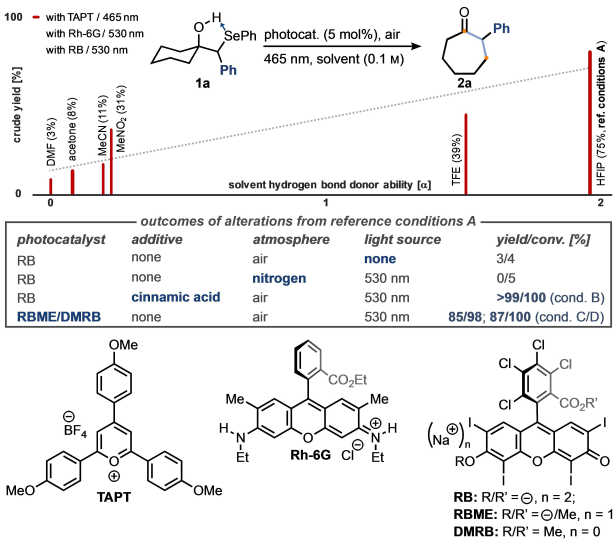

Scheme 4. Reaction optimization for H-bond-modulated, photoredox catalytic type I semipinacol rearrangement. Screening of photocatalysts and solvents as well as correlation of the reaction yield with the Kamlet-Taft α-parameters of various solvents. Dotted line corresponds to regression line (R^2 = 0.84) of all experiments involving TAPT as the photocatalyst.

Investigation continued with the exploration of the substrate scope (Schemes 5 and 6). The photo-aerobic rearrangement proved effective for the synthesis of a wide array of cyclic and acyclic ketones **2** (Scheme 5). For example, α-monoarylated cycloalkanones **2a**–**e**, possessing ring sizes between 7–10 members, were obtained in yields ranging from 53 % to 93 %. Also, aliphatic ketones **2f**–**m** with α,α-, α,α′- and α,β-disubstitution were accessible in up to 98 % yield. These observations are notable for two reasons: 1) Krief et al. stated in one of their investigations that the migratory fragmentations of selenohydrins occur only with substrates in which the selenium residue is bound to a tertiary carbon atom.[19] Thus, in contrast to our photo-aerobic protocol, only ketones with geminal disubstitution at the α-position are accessible by this and related methods.[21,22] In the case of selenohydrins **2f**, **2g** and **2s**, the migratory aptitude of the methylene group was higher than that of tertiary and quaternary moieties. This site selectivity is in agreement with cognate type I semipinacol rearrangements,[18] in which the migratory preference is governed by stereoelectronic factors. In light of this analogy, we concluded that the observed site selectivity might be the result of a H-bond-assisted conformational bias present in the respective precursors, which orient the C–Se σ-bond in a dihedral angle of about 180° relative to the migrating fragment.[35,36] Consequently, despite the increased reactivity of the selenohydrins under photo-aerobic conditions there is no observable loss in stereospecificity. Our photo-aerobic semipinacol protocol also tolerated several heteroatomic entities, such as ethers, unprotected hydroxyl, amino, and sulfur groups (i.e. **2o**–**r**, **2u**), and was suitable for the

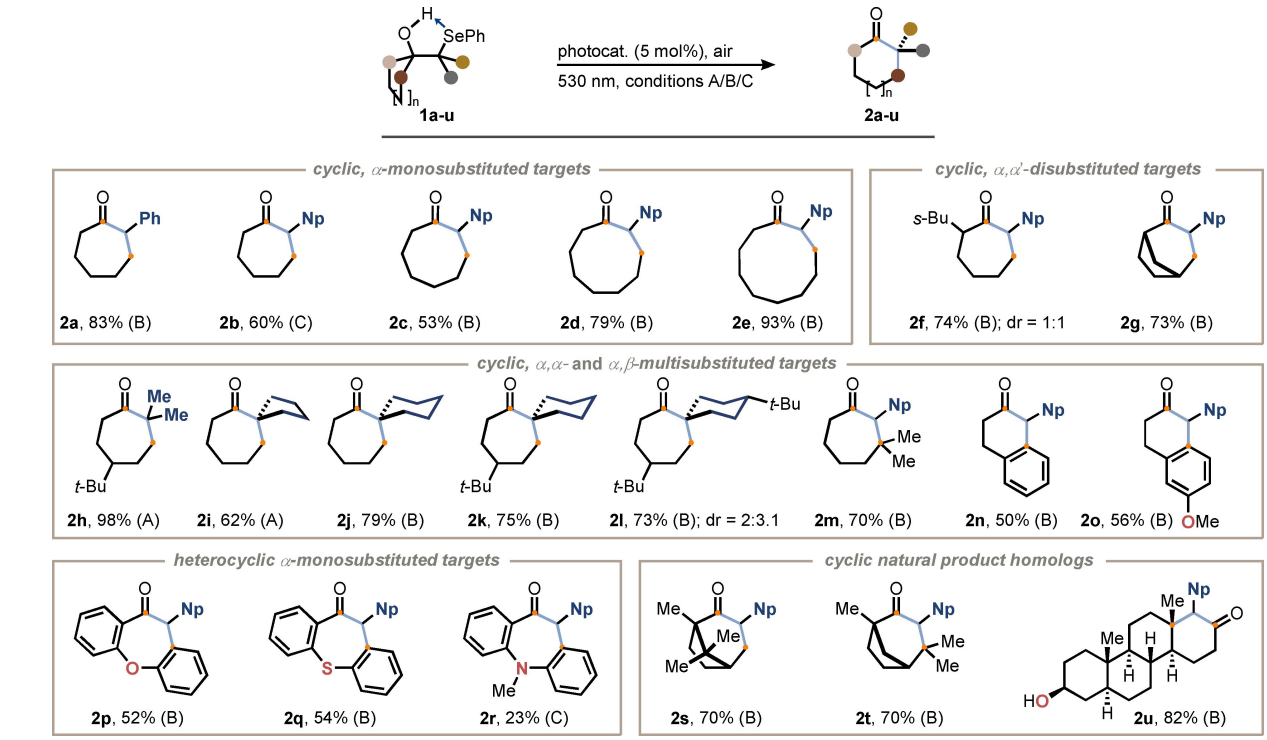

Scheme 5. Reaction scope—cyclic ketones. All reactions took place in HFIP (0.1 M) with 1.0 mmol of **1** under 530 nm irradiation for 2 h at temperatures between 19 °C and 23 °C. For the depicted products **2** the following catalysts and additives were used: conditions A (photocat. = RB (5 mol%)), conditions B (photocat. = RB (5 mol%), cinnamic acid (50 mol%)), conditions C (photocat. = RBME (5 mol%)). Yields refer to isolated compounds. Np = 2-naphthyl.

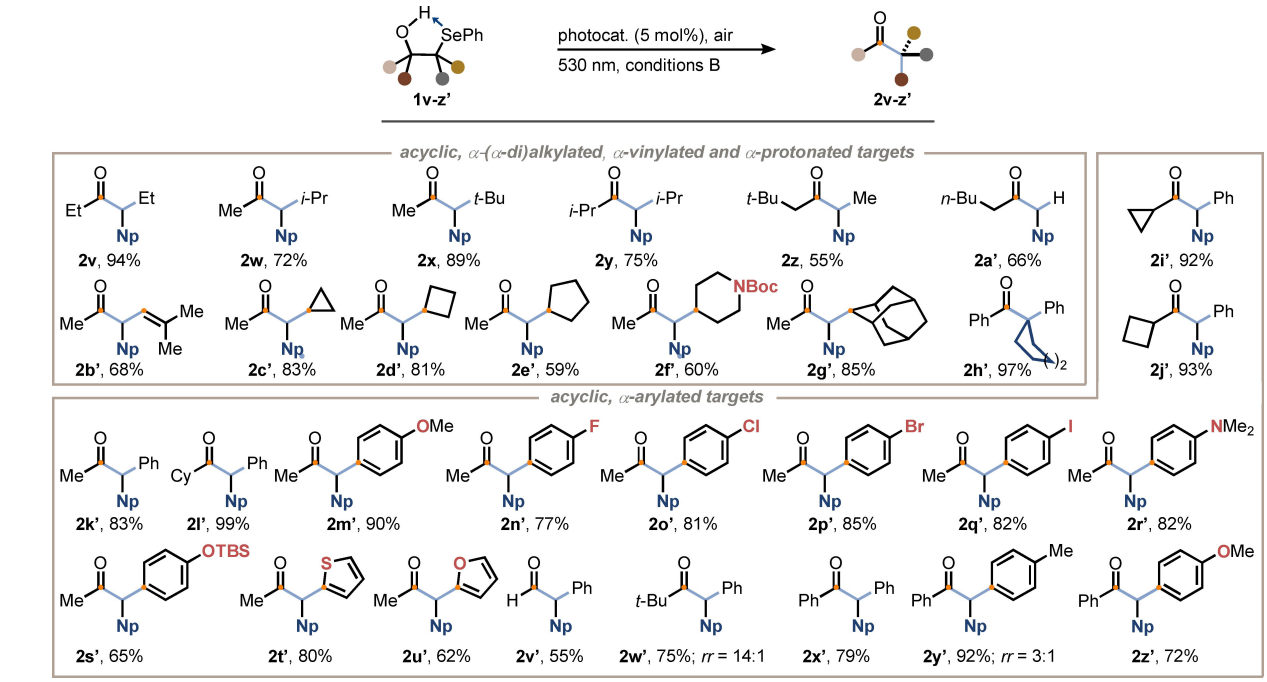

Scheme 6. Reaction scope—acyclic ketones. All reactions took place in HFIP (0.1 M) with 1.0 mmol of **1** under 530 nm irradiation for 2 h at temperatures between 19 °C and 23 °C. For the depicted products **2** 5 mol% of RB and 50 mol% cinnamic acid (conditions B) were used. Yields refer to isolated compounds. Np = 2-naphthyl, *rr* = regioisomeric ratio.

formation of sterically highly congested fenchone homolog **2t**.

To explore the utility of the title protocol regarding functional group tolerance and migratory preferences, a structurally diverse series of selenohydrins **1v–z′** was subjected to the title conditions (Scheme 6). Selenohydrins **1v–z**, which possess two aliphatic groups with varying steric demand at the carbinol C-atom, smoothly converted into target compounds **2v–z** in yields ranging between 55 % to 94 %. In these cases, a typical migratory preference for the sterically more demanding alkyl group was observed. This outcome was independent of any torsional strain within the migrating groups, as was observed in a representative set of cycloalkylated selenohydrins **1c′–e′**. Comparison of the migratory aptitudes of alkyl vs. aryl groups (i.e., **2i′–u′**) showed that arenes exhibited a higher preference for migration, even when a *tert*-butyl moiety was employed as a competing group (**2w′**, 14:1 inferior to a phenyl group). The only product with a counter-intuitive migratory aptitude is ketone **2z**, in which the methyl group migrated preferentially, presumably due to a conformational bias within **1z**. Bis-arylated substrates **1x′–z′** showed a strong electronic migratory preference in favor of the more electron rich aryl groups (**2x′–z′**). Eventually, 1,2-disubstituted selenohydrins **1a′** and **1v′** were tested, which were derived from the corresponding aldehydes. In those experiments, migration of the hydrogen atom was superior to the alkyl moiety but inferior to a phenyl group (cf. **2a′** and **2v′**). Looking at the synthetic results in total, the title method is effective for tetra-, tri-, and disubstituted selenohydrins, which provides a facile access to rearranged α-mono- and α,α-disubstituted ketones as well as ketones from aldehydes. In addition, the protocol is compatible with common functional groups, such as halogens, amines, carbamates, (silyl)ethers, and heterocycles, thus, showcasing a very broad synthetic utility.

To unravel the impact of HFIP in more detail, broadband transient absorption studies on a ns to ms timescale were performed.[37] Excitation of selenohydrin **1a″** (Supporting Information, Figures S23–S26) with laser pulses at 355 nm disclosed a strongly solvent-dependent photolysis. In DCM, an intermediate absorbing between 400 nm and 500 nm was recorded, whereas in HFIP a signal above 650 nm was observed. We presumed that radical formation takes place in both solvents yet by different mechanisms for the carbon-selenium bond cleavage. We thus attempted to identify the suspected intermediates by photolysis of $(PhSe)_2$. The spectra of the resulting phenylselenyl radicals[37,38] were previously reported with a characteristic absorption below 500 nm[39–42] in various solvents, albeit not in HFIP. Upon excitation of $(PhSe)_2$ in both DCM and HFIP, the signal of PhSe$^\bullet$ decayed with second-order kinetics on a sub-ms timescale to regenerate $(PhSe)_2$ (Scheme S27–29). However, when methanesulfonic acid (MSA) was added as a proton source to a HFIP solution of $(PhSe)_2$, photo-generated PhSe$^\bullet$ converted into PhSeH$^{\bullet+}$, as is evident from identical decay and rise times of the respective spectral signatures (Scheme S33), with the feature above 650 nm (Scheme 7, center) being in very good agreement with transient spectra of PhSeH$^{\bullet+}$ generated by pulsed radiolysis as reported by Brede et al.[41] Consequently, the species formed when exciting **1a″** in HFIP could be unequivocally identified as the PhSeH$^{\bullet+}$ radical cation. We then analyzed the title reaction by transient absorption spectroscopy with 532 nm excitation of DMRB ($c = 18$ μM) in the presence of a 6000-fold excess of substrate **1a** (108 mM). Whereas neither reactant **1a** nor product **2a** does absorb above 300 nm, three characteristic transient features (ocher spectra, Scheme 7) unveiled the mechanism of this photoreaction: 1) the DMRB ground-state bleach persists on the monitored timescale, thus excited DMRB molecules do not recover directly but rather take up an electron from the substrate. 2) A sharp absorption peak at 375 nm originates from the resulting DMRB radical anion,[43] whose identity was independently verified by reducing DMRB with benzylphenylselenide (Scheme 7, right). 3) The absorption above 650 nm is identical to that of PhSeH$^{\bullet+}$ (Scheme 7,

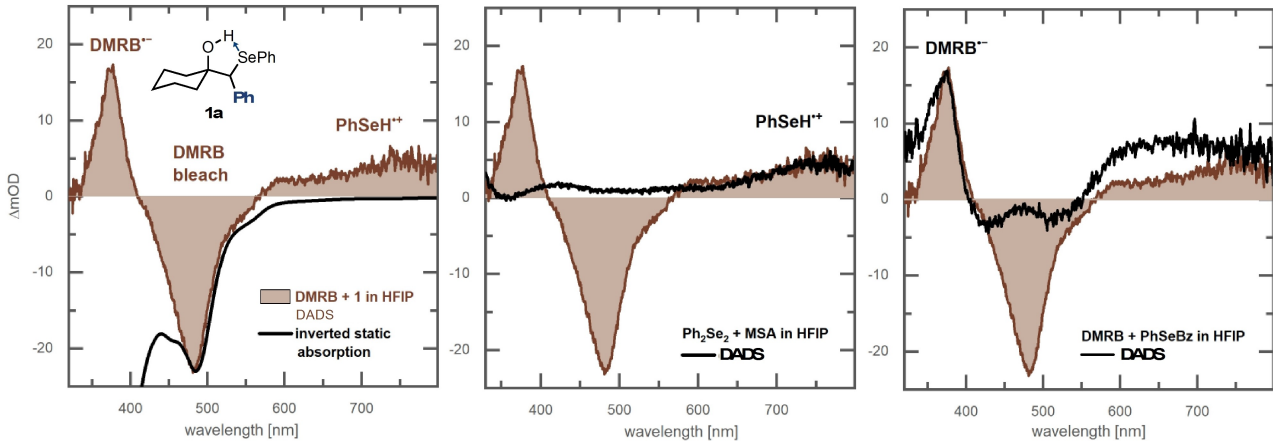

Scheme 7. Laser spectroscopic investigation of the rearrangement reaction. Decay-associated difference spectrum (DADS) from transient absorption experiments corresponding to signals persisting for times well beyond 10 μs (see Supporting Information for complete data range). The data for exciting DMRB (18 μM) in the presence of **1a** (108 mM) is shown in ocher in all three panels. Comparison to three separate experiments (scaled black spectra) discloses the signal contributions of DMRB bleach, PhSeH$^{\bullet+}$, and DMRB$^{\bullet-}$, respectively.

center and ref. [41]), corroborating the occurrence of this particular radical cation under catalytic conditions. Since PhSe• is not protonated in neat HFIP, but can be in the presence of an additional proton source (such as methanesulfonic acid, vide supra), we conclude that in the course of the title reaction a proton is intramolecularly transferred from the OH group of the selenohydrin to the adjacent, hydrogen-bonded Se-atom during the C–Se bond cleavage. This process becomes increasingly feasible with a growing H-bond donor ability of the solvent, and is optimal in HFIP. Additional EPR studies on the direct excitation of **1b″** in HFIP led to the resonance signature shown in Scheme 8b. The g-value of 2.026 is in good agreement with related ArSeR•+ species,[44] but significantly larger than g-values reported for PhSe• (2.003, 2.016).[45,46] We therefore speculate that the role of the solvent is to compensate the negative charge build-up at the O-atom during the proton transfer from oxygen to selenium through intermolecular H-bonding. Consequently, our time-resolved spectroscopic data, in combination with the results from the NMR experiments mentioned above, strongly support a multisite proton-coupled electron transfer (PCET)[47,48] as the key mode of action.

Finally, a computational analysis (DFT, see Supporting Information for details) of the reaction mechanism was performed to address the following questions: (1) does the C–Se bond scission take place mesolytically (Scheme 8, pathway I) or homolytically (pathways II and III) upon the photocatalytic SET event, (2) are the O–H and C–Se bond cleavages occurring sequentially (pathways I and II) or concertedly (pathway III), and (3) if a sequential mechanism is operative, does the C–Se bond cleavage precede the proton transfer (pathway I) or does a hydrogen atom transfer (HAT) from the OH group onto the Se-centered radical cation takes place first (pathway II, i.e. inverted sequential)? Each of these aspects may allow to rationalize the critical role of the protic polar environment and the intramolecular OH···Se H-bond. First, a differentiation between the mesolytic and homolytic C–Se bond scission pathways was carried out. In principle, either of the two bond cleavage pathways may lead to the spectroscopically characterized PhSeH•+ and target compound **2a** (i.e., Schemes 7a and 8b). Thus, a relaxed scan of the potential

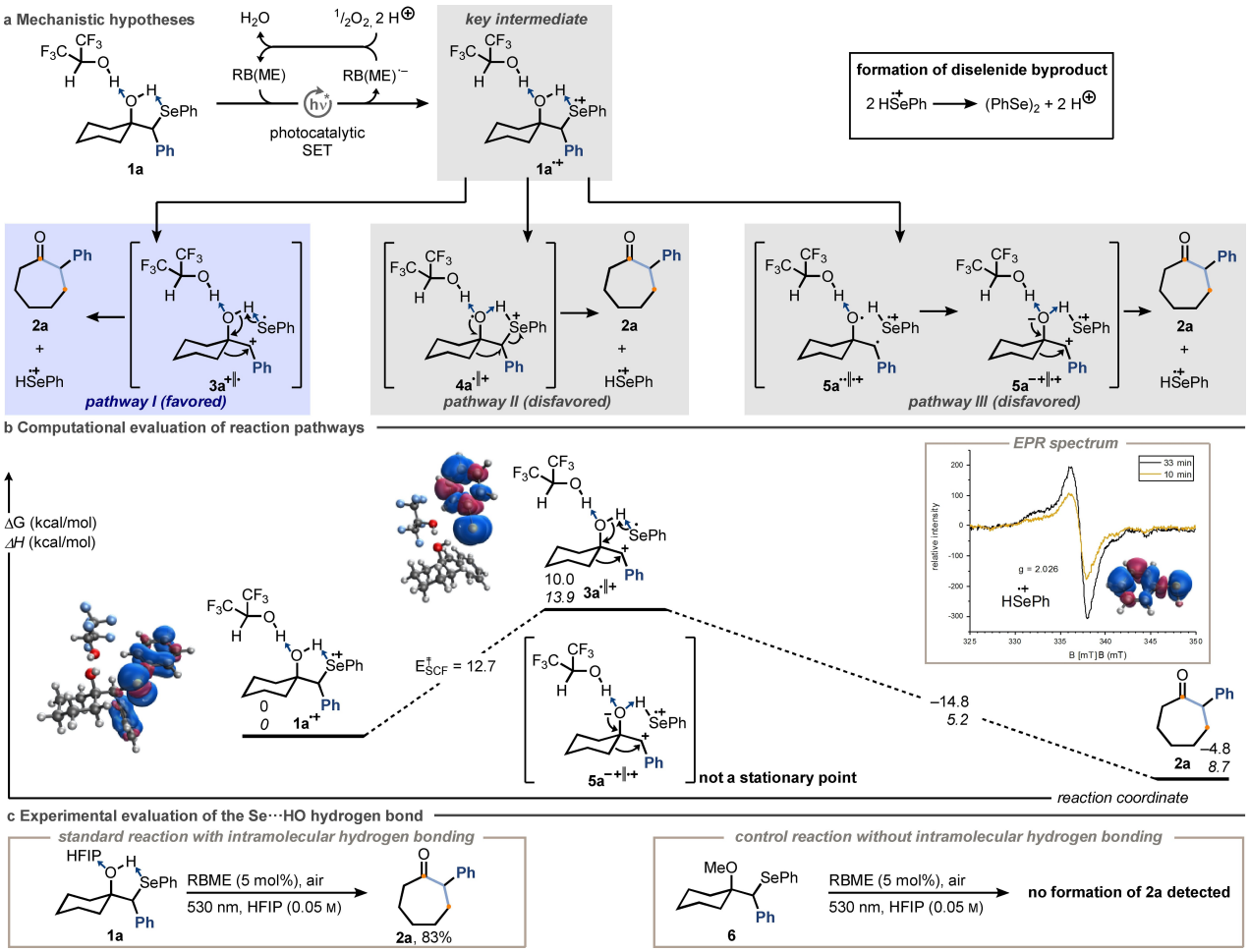

Scheme 8. Mechanistic postulate based on experimental and computational data. a) comparison of possible reaction pathways leading from 1 to 2. b) thermodynamic evaluation of reactive intermediates by DFT calculations. c, control experiment for the evaluation of the significance of the intramolecular Se···HO hydrogen bond.

energy surface created by extending the C–Se bond length in the [HFIP···**1a**$^{\bullet+}$] complex[49] revealed that dissociation of the C–Se bond is a facile process ($E_{SCF}^{\neq}$ = 12.4 kcal mol^{-1}). NBO analysis along that scanned path and of the fully optimized and confirmed starting and final minimum energy structure of [HFIP···**1a**$^{\bullet+}$] and [HFIP···**3a**$^{\bullet||+}$] ($\Delta_R G$ = 10.0 kcal mol^{-1}), respectively, indicate a *mesolytic* bond cleavage. Consequently, the intermediates instantly formed in this step are carbocation **3a**$^{+}$ and PhSe$^{\bullet}$, which remain H-bonded to one another. At the outset, complex [HFIP···**3a**$^{\bullet||+}$] does not show any O–H bond elongation (path I, Scheme 8a), but with a continuously emerging separation of the spin and charge (plotted spin densities in Scheme 8b, for partial charge analysis, see Supporting Information, Figure S39) the intramolecular H-bond interactions to the Se-atom increases, leading to a net-stabilization of 2.4 kcal mol^{-1} in comparison to the separated PhSe$^{\bullet}$ and **3a**$^{+}$. The ensuing step toward target product **2a** makes a proton transfer from **3a**$^{+}$ to PhSe$^{\bullet}$ necessary, which would formally lead to zwitterionic structure [HFIP···**5a**$^{+-||\bullet+}$]. However, this zwitterion was not a stationary point on the PES. Instead, with removal of the proton from carbocation **3a**$^{+}$, the path is exothermic toward target product **2a** and PhSeH$^{\bullet+}$. This analysis is congruent with the hypothesis that HFIP may compensate negative charge build-up on the O-atom of fragment **3a**$^{+}$.

A related 2D-scan, built from driving the O–H bond and the C–Se bond length concertedly, delivered additional information on the alternative pathways II and III. Both alternative pathways are significantly higher in energy with barriers beyond 35 kcal mol^{-1} (Supporting Information, Figure S40), mostly due to the endothermicity of the HAT. An interesting aspect of the 2D-scan was obtained regarding the on-set of the rearrangement of the carbon framework. Analysis of geometric parameters (Supporting Information) along the different scanned structures indicated that neither the O–H nor the C–Se bond cleavage is sufficient on its own to induce conformational changes within the carbon framework. In other words, upon mesolytic C–Se bond scission the proton transfer is accompanied by the 1,2-carbon shift. This notion implies that in the absence of a transferable proton between the O- and Se-atom, the 1,2-carbon shift should not occur. Thus, *O*-methylated analog **6** (Scheme 8c, right) was synthesized and subjected to the title conditions. Notably, after a reaction time of 2 h there was no formation of ketone **2a** detected, which is in agreement with the computational prediction. Instead, selenide **6** was turned into its corresponding selenoxide (Supporting Information, compound **S4**, Figure S2b). To check whether cognate selenohydrin oxides, potentially formed in situ from selenohydrins **1**, may play a role in the catalytic cycle, we synthesized selenohydrin oxide **S6** (Supporting Information, Figures S2c and S2d) from selenohydrin **1a** and analyzed its conversion under the title conditions. It turned out that selenohydrin oxide **S6** indeed can also react to ketone **2a**, albeit with significantly altered kinetics, as was evident from 1H NMR-spectroscopy-based initial rate studies (Supporting Information, Figures S2c to S2h). From the body of these observations, in combination with the transient absorption spectroscopic data (Scheme 7, left and central spectra) and computational findings, it can be concluded that the title reaction most likely proceeds through catalytic pathway I.

Conclusion

In conclusion, we have shown for the first time that the nucleofugality of selenium residues can be modulated by the combination of single electron oxidation and OH···Se H-bond interactions to switch from an archetypical elimination pathway to a substitution manifold. This activation principle has been successfully implemented in an unprecedented photoredox catalytic type I semipinacol rearrangement of selenohydrins **1** to provide access to a structurally diverse array of ketones **2** in good to excellent yields and with outstanding selectivity. This unusual mode of Se–C bond activation and its implications for the catalytic cycle was elucidated by NMR, EPR and transient absorption spectroscopy as well as computational methods. From a broader perspective, our findings are expected to have significant consequences for the synthetic exploitation of H-bond interactions involving heavy, less electronegative acceptor atoms such as selenium and related elements—in particular in combination with photochemical means—to create reactivity profiles that are as yet elusive.

Acknowledgements

We thank R. J. Kutta, E. Harrer, D. Grenda (University of Regensburg) for technical and operational support. Funding: We thank the European Research Council (ERC Starting Grant "ELDORADO", grant agreement No. 803426), the German Research Foundation (DFG, RTG 426795949), and the Studienstiftung des deutschen Volkes for financial support. Furthermore, the project was funded by the Deutsche Forschungsgemeinschaft (DFG, German Research Foundation)—TRR 325-444632635. Open Access funding enabled and organized by Projekt DEAL.

Conflict of Interest

The authors declare no conflict of interest.

Data Availability Statement

The data that support the findings of this study are available in the Supporting Information of this article.

Keywords: Hydrogen-Bonds · Nucleofugality · Photoredox-Catalysis · Rearrangements · Selenium(III)

[1] L. J. Prins, D. N. Reinhoudt, P. Timmerman, *Angew. Chem. Int. Ed.* **2001**, *40*, 2382–2426; *Angew. Chem.* **2001**, *113*, 2446–2492.

[2] A. G. Doyle, E. N. Jacobsen, *Chem. Rev.* **2007**, *107*, 5713–5743.
[3] P. R. Schreiner, *Chem. Soc. Rev.* **2003**, *32*, 289–296.
[4] M. S. Taylor, E. N. Jacobsen, *Angew. Chem. Int. Ed.* **2006**, *45*, 1520–1543; *Angew. Chem.* **2006**, *118*, 1550–1573.
[5] X. Yu, W. Wang, *Chem. Asian J.* **2008**, *3*, 516–532.
[6] T. Nakamura, K. Okuno, R. Nishiyori, S. Shirakawa, *Chem. Asian J.* **2020**, *15*, 463–472.
[7] V. R. Mundlapati, D. K. Sahoo, S. Ghosh, U. K. Purame, S. Pande, R. Acharya, N. Pal, P. Tiwari, H. S. Biswal, *J. Phys. Chem. Lett.* **2017**, *8*, 794–800.
[8] A. Chand, D. K. Sahoo, A. Rana, S. Jena, H. S. Biswal, *Acc. Chem. Res.* **2020**, *53*, 1580–1592.
[9] A. Chand, H. S. Biswal, *J. Indian Inst. Sci.* **2020**, *100*, 77–100.
[10] M. Iwaoka, S. Tomoda, *J. Am. Chem. Soc.* **1994**, *116*, 4463–4464.
[11] L. Engman, *J. Org. Chem.* **1987**, *52*, 4086–4094.
[12] A. M. Morella, A. D. Ward, *Tetrahedron Lett.* **1984**, *25*, 1197–1200.
[13] A. M. Morella, A. D. Ward, *Tetrahedron Lett.* **1985**, *26*, 2899–2900.
[14] A. J. Cresswell, S. T.-C. Eey, S. E. Denmark, *Nat. Chem.* **2015**, *7*, 146–152.
[15] Z. Tao, B. B. Gilbert, S. E. Denmark, *J. Am. Chem. Soc.* **2019**, *141*, 19161–19170.
[16] E. M. Mumford, B. N. Hemric, S. E. Denmark, *J. Am. Chem. Soc.* **2021**, *143*, 13408–13417.
[17] J. R. Tabor, D. C. Obenschain, F. E. Michael, *Chem. Sci.* **2020**, *11*, 1677–1682.
[18] Z.-L. Song, C.-A. Fan, Y.-Q. Tu, *Chem. Rev.* **2011**, *111*, 7523–7556.
[19] J. L. Laboureur, A. Krief, *Tetrahedron Lett.* **1984**, *25*, 2713–2716.
[20] D. Labar, J. L. Laboureur, A. Krief, *Tetrahedron Lett.* **1982**, *23*, 983–986.
[21] L. A. Paquette, J. R. Peterson, R. J. Ross, *J. Org. Chem.* **1985**, *50*, 5200–5204.
[22] F. Löhr, S. G. Mayhew, H. Rüterjans, *J. Am. Chem. Soc.* **2000**, *122*, 9289–9295.
[23] H.-J. Sass, F. Fang-Fang Schmid, S. Grzesiek, *J. Am. Chem. Soc.* **2007**, *129*, 5898–5903.
[24] N. Sorgenfrei, J. Hioe, J. Greindl, K. Rothermel, F. Morana, N. Lokesh, R. M. Gschwind, *J. Am. Chem. Soc.* **2016**, *138*, 16345–16354.
[25] S. Sharif, G. S. Denisov, M. D. Toney, H-.H. Limbach, *J. Am. Chem. Soc.* **2007**, *129*, 6313–6327.
[26] R. M. Gschwind, M. Armbrüster, I. Z. Zubrzycki, *J. Am. Chem. Soc.* **2004**, *126*, 10228–10229.
[27] G. Federwisch, R. Kleinmaier, D. Drettwan, R. M. Gschwind, *J. Am. Chem. Soc.* **2008**, *130*, 16846–16847.
[28] R. Kleinmaier, M. Keller, P. Igel, A. Buschauer, R. M. Gschwind, *J. Am. Chem. Soc.* **2010**, *132*, 11223–11233.
[29] A. Berkessel, J. A. Adrio, D. Hüttenhain, J. M. Neudörfl, *J. Am. Chem. Soc.* **2006**, *128*, 8421–8426.
[30] Due to conformational issues of the non-planar five membered ring, the simulation showed two very similar orientations of the OH group corresponding to both sides of the ring.
[31] M. Martiny, E. Steckhan, T. Esch, *Chem. Ber.* **1993**, *126*, 1671–1683.
[32] M. Wilken, S. Ortgies, A. Breder, I. Siewert, *ACS Catal.* **2018**, *8*, 10901–10912.
[33] M. J. Kamlet, J.-L. M. Abboud, M. H. Abraham, R. W. Taft, *J. Org. Chem.* **1983**, *48*, 2877–2887.
[34] C. Reichardt, T. Welton, *Solvents and Solvent Effects in Organic Chemistry*, 4th ed., Wiley-VCH, Weinheim, **2011**.
[35] J. L. Laboureur, A. Krief, *Tetrahedron Lett.* **1987**, *28*, 1545–1548.
[36] A. Krief, J. L. Laboureur, G. Evrard, B. Norberg, E. Guittet, *Tetrahedron Lett.* **1989**, *30*, 575–576.
[37] R.-J. Kutta, T. Langenbacher, U. Kensy, B. Dick, *Appl. Phys. B* **2013**, *111*, 203–216.
[38] E. N. Deryagina, M. G. Voronkov, N. A. Korchevin, *Russ. Chem. Rev.* **1993**, *62*, 1107–1117.
[39] O. Ito, *J. Am. Chem. Soc.* **1983**, *105*, 850–853.
[40] P. Beletskaya, A. S. Sigeev, V. A. Kuzmin, A. S. Tatikolov, L. Hevesi, *J. Chem. Soc. Perkin Trans. 2* **2000**, 107–109.
[41] O. Brede, R. Hermann, S. Naumov, H. S. Mahal, *Chem. Phys. Lett.* **2001**, *350*, 165–172.
[42] S. Tojo, M. Fujitsuka, A. Ouchi, T. Majima, *ChemPlusChem* **2015**, *80*, 68–73.
[43] C. Lambert, T. Sarna, T. G. Truscott, *J. Chem. Soc. Faraday Trans.* **1990**, *86*, 3879–3882.
[44] S. Zhang, X. Wang, Y. Su, Y. Qiu, Z. Zhang, X. Wang, *Nat. Commun.* **2014**, *5*, 4127.
[45] J. J. Windle, A. K. Wiersema, A. L. Tappel, *J. Chem. Phys.* **1964**, *41*, 1996–2002.
[46] E. N. Deryagina, M. G. Voronkov, *Sulfur Rep.* **1995**, *17*, 89–123.
[47] J. J. Warren, T. A. Tronic, J. M. Mayer, *Chem. Rev.* **2010**, *110*, 6961–7001.
[48] D. C. Miller, K. T. Tarantino, R. R. Knowles, *Top. Curr. Chem. (Z)* **2016**, *374*, 30.
[49] Radical cations $\mathbf{1}^{\bullet+}$ are formed by a SET with photoexcited (DM)RB(ME) (Scheme 8a), giving the corresponding reduced photocatalyst. This latter species is believed to be re-oxidized by aerial O_2 to reach its original oxidation state and re-enter the catalytic cycle. For a mechanistic study on related photo-aerobic selenium-π-acid catalyzed alkene functionalizations, see: S. Ortgies, R. Rieger, K. Rode, K. Koszinowski, J. Kind, C. M. Thiele, J. Rehbein, A. Breder, *ACS Catal.* **2017**, *7*, 7578–7586.

Manuscript received: June 12, 2022
Accepted manuscript online: September 16, 2022
Version of record online: ■■, ■■

Research Articles

Photocatalysis

S. Park, A. K. Dutta, C. Allacher, A. Abramov, P. Dullinger, K. Kuzmanoska, D. Fritsch, P. Hitzfeld, D. Horinek, J. Rehbein,* P. Nuernberger,* R. M. Gschwind,* A. Breder* e202208611

Hydrogen-Bond-Modulated Nucleofugality of Se^{III} Species to Enable Photoredox-Catalytic Semipinacol Manifolds

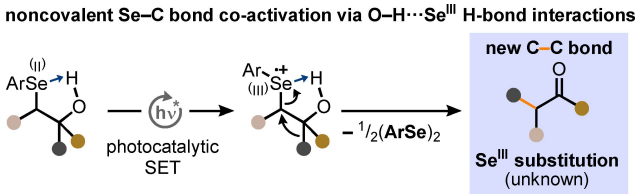

A photoredox catalytic 1,2-carbon-shift manifold is enabled by an unprecedented OH···Se^{III} hydrogen bond co-activation of C–Se σ-bonds. While traditional oxidative methods for the activation of C–Se σ-bonds proceed through Se^{IV} intermediates and commonly result in rapid elimination of the Se^{IV} residue, this protocol facilitates, for the first time, the stereospecific substitution of Se^{III} nucleofuges by carbon nucleophiles.